

Submitted:
30.04.2021
Accepted:
28.06.2021
Published:
29.11.2021

Diagnostic value of 12-zone lung ultrasound protocol for diagnosing COVID-19-associated pneumonia in outpatients

Dzmitry Haurylenka¹, Victor Damantsevich²,
Andrey Filustsin², Anna Damantsevich²

¹ Functional Diagnostic Department, State Institution Republican Research Centre for Radiation Medicine and Human Ecology, Belarus

² Radiology Department, State Institution Republican Research Centre for Radiation Medicine and Human Ecology, Belarus

Correspondence: Dzmitry Haurylenka, Functional Diagnostic Department, State Institution Republican Research Centre for Radiation Medicine and Human Ecology, 246040, st. Ilyicha, 290, Gomel, Belarus, tel.: +375232389927; e-mail: dm.gavrilenko891@gmail.com

DOI: 10.15557/JoU.2021.0046

Keywords

subpleural consolidation, lung ultrasound, COVID-19

Abstract

Introduction: In the SARS-CoV-2 pandemic, lung ultrasound can be of decisive importance for planning further treatment approach in patients with infection. There is still no clear priority for the choice of lung ultrasound protocol in an outpatient setting. **Aim:** The objective of the study was to evaluate the applicability of 12-zone protocol lung ultrasound for the diagnosis of COVID-19 associated pneumonia in outpatients. **Materials and methods:** We examined 39 outpatients meeting the diagnostic criteria of COVID-19 infection (17 men and 22 women) aged 31–75 years (median 49 years). All patients underwent lung ultrasound immediately after chest computed tomography performed by a blinded specialist. Correlation analysis of the results of a quantitative assessment of the detected signs, assessment of the diagnostic significance of lung ultrasound for identifying signs of pneumonia were performed. **Results:** Pneumonia was diagnosed by computed tomography in 25 (64%; 95% CI 47–79) out of 39 patients. At the same time, ultrasound signs of interstitial abnormalities were detected in 31 patients. Multiple (narrow) B-lines, confluent (wide) B-lines, as well as areas of subpleural consolidation and “white lung” were the most common lung ultrasound abnormalities. When evaluating the method, the optimal sensitivity/specificity ratio was obtained for a value of ≥ 2 points, the area under the curve = 0.970 (95% CI 0.858–0.999; $p < 0.0001$). The score of lung ultrasound significantly correlated with computed tomography quantitative assessment ($r = 0.928$, $p < 0.001$). **Conclusion:** Despite some limitations, lung ultrasound can be extremely useful in primary care settings, also in the case of a significant number of admitted patients, to detect features of COVID-19 associated pneumonia.

Introduction

The main methods for diagnosing pathological changes in the chest organs of patients with suspected pneumonia is chest X-ray and, in the case of COVID-19-associated pneumonia, chest computed tomography (CT). The choice of imaging method is determined by the technical capabilities (equipment) and human resources of the healthcare institution, as well as number of incoming patients.

Standard chest X-ray can be used if it is technically impossible to perform CT, as it has poor sensitivity in

detecting changes at the initial stage of COVID-19-associated lesions⁽¹⁾. The informative value of chest X-ray increases in patients with severe pneumonia, at a late stage of the process; also, this method has sufficient sensitivity for the diagnosis of pulmonary edema⁽²⁾. A mobile X-ray unit can be used for patients of the intensive care unit, though it has its own limitations of informativeness. Thus, one of the few advantages of standard chest X-ray is the high patient throughput due to the examination duration.

Computed tomography is in fact the „gold standard“ method for detecting lung tissue changes in COVID-19

associated pneumonia. CT chest scan is optimal for the initial assessment of chest organs if there are severe clinical signs of COVID-19 infection^(1,3). The method is indispensable for the differential diagnosis of causes in severe respiratory failure. The main limitations of chest CT are the technical complexity of the examination of patients who are on mechanical ventilation, higher (in comparison with chest X-ray) exposure, and lower patient throughput. It should be considered that the changes revealed by CT chest scan are not highly specific in relation to the etiological factor of the pathological process⁽⁴⁾. In other words, despite the existence of a number of CT patterns, this method, as well as other imaging methods, should be followed by laboratory testing for COVID-19 infection. CT chest scan is not recommended for screening, including cases with positive laboratory tests for COVID-19 infection⁽⁵⁾.

A number of static and dynamic signs can be detected with lung ultrasound (LUS). Lung ultrasound provides imaging based on both "true" images and artifacts. In fact, a "true" image of the lung tissue is created only in areas where air is completely absent (consolidation), that is lung pathology sign. The presence of air in the subpleural parenchyma, on the other hand, creates image artifacts associated with the reflection and reverberation of the ultrasound wave. Ultrasound of a normal lung does not visualize true images outside the pleural layers, but it is possible to identify various types of artifacts associated with reverberation. The key factor that determines the current appearance of the visualized area is the "air/fluid ratio" in the subpleural lung parenchyma⁽⁶⁾. This ratio determines the following visual findings: 1) normally ventilated lung – forms a homogeneous reflective surface that forms transverse artifacts

parallel to the pleural line „line A“; 2) partial loss of airiness – due to infiltration by liquid and/or cells in the subpleural layer of the lung tissue, clearly delineated microscopic three-dimensional aerated structures (aerated alveoli and/or acini surrounded by fluid or cells) are formed, which are reflectors of ultrasonic waves and sources of reverberation, which leads to the appearance of longitudinal signals of the „comet's tail" type – „B-lines" type; 3) the complete absence of air even in small areas under the visceral pleura (subpleural consolidation) provides favorable conditions for the transmission of ultrasound with partial reflection, the lung tissue is visualized as a solid organ^(2,6,7).

Aeration can be decreased due to air loss – the development of atelectasis, fluid accumulation, or cellular infiltration of the interstitial and/or alveolar space (pneumonia, edema, fibrosis, or alveolitis), which creates abnormal nonspecific profiles detected at lung ultrasound.

Aim

To evaluate the diagnostic value and applicability of a 12-zone protocol for LUS in outpatients with pneumonia associated with COVID-19 infection.

Material and methods

The study was approved by the Local Ethics Committee (protocol No.8 dated 12 Nov 2020).

The study included 39 outpatients meeting the diagnostic criteria for COVID-19 infection (17 men and 22 women) at the age of 31–75 years (median 49 years), who had a chest CT performed in the period from November to December 2020.

The SARS-CoV-2 infection was confirmed through reverse transcriptase polymerase chain reaction in nasopharyngeal swab, which was performed in all patients according to WHO standards⁽⁸⁾.

In addition to laboratory confirmation of SARS-CoV-2 infection, all 39 patients had clinical signs indicating acute respiratory infection. The most common symptoms were fever, cough with/without sputum, dyspnea. The baseline characteristics of the patients included in the study are presented in Tab. 1.

Chest CT scan was adopted as the reference method for diagnosing pneumonia. Chest multidetector scanning was performed according to a standard protocol, using a DISCOVERY 750 HD (General Electric, USA) machine. The scanning parameters were as follows: tube voltage = 120 kV, automatic mA setting on basis of patient size, automatic tube current modulation; pitch = 1; matrix = 512 × 512; collimation = 0.625 mm. The images were reconstructed with slice thickness = 5 and 1.25 mm using a pulmonary and a mediastinal kernel. The patient was in the supine position with their hands behind their head, during

Tab. 1. Basic demographic and clinical data of patients included in the study

Variables	Patients, n = 39
Age, years, Me [Q1; Q3]	49 [39; 61]
Gender, male/female (%)	17 (44) / 22 (56)
Symptoms (%; 95% CI):	
fever	35 (90; 76–97)
cough	26 (67; 50–81)
sputum	12 (31; 17–48)
dyspnea	18 (46; 30–63)
chest pain	7 (18; 8–34)
anosmia	7 (18; 8–34)
sweating	5 (13; 4–27)
Oxygen saturation, %, Me [min; max]	98 [82; 90]
Symptom duration, days, Me [min; max]	9 [3; 30]
No comorbidities. (%; 95% CI)	16 (41; 26–58)
Comorbidities, Me [min; max]:	2 [1; 5]
Hypertension:	16
Stage 1	7
Stage 2	7
Stage 3	2
Obesity	11
Non-alcoholic fatty liver disease	9
Cardiovascular disease	6
Diabetes	4
Chronic bronchitis	3
Chronic kidney disease	2
Post-stroke period	1

Tab. 2. The borders of the examined areas in accordance with the segments anatomical landmarks

		Side							
		posterior		lateral		anterior		I. parasternalis	
		right	left	right	left	right	left		
Upper	I. paravertebralis	S1, S2, S6	S1, S2, S6	I. axillaris posterior	S1, S2, S3, S4	S1, S2, S3, S4, S6	I. axillaris anterior	S1, S3	S1, S3, S4
Lower		VI edge			V edge			IV edge	
		S6, S10, S9	S10		S4, S8	S8, S9, S10		S4, S5, S8	S4, S5, S8

a breath-hold. The scanned areas were divided into 12 zones in such a way that they included the corresponding 12 zones of the lung ultrasound protocol. Each scanning area was assigned a score from 0 to 3 based on the prevalent lesion patterns: normal = 0; “ground-glass” opacity = 1; interstitial changes = 2; consolidation = 3⁽⁹⁾.

Lung ultrasound was performed within 15–20 minutes after CT scan by a blinded specialist on a Vivid E9 system (General Electric, Norway) using a convex probe (frequency 1.8–6.0 MHz) in a sitting position (on a medical exam stool). The LUS image analysis was performed in the Diagnostic Department by an experienced clinician with an assessment of changes in 12 chest zones - 6 on the left and 6 on the right (Tab. 2). The abnormalities in the lung profile were recorded in each of the 12 zones of the protocol, scored from 0 to 3 according to Soldati *et al.*⁽⁷⁾: the pleural line is continuous, horizontal artifacts referred to as A-lines are detected due to the reflectivity of the normal aerated subpleural lung surface = 0; >3 clearly separated B-lines in the field = 1 point; wide B-lines or coalescing into a „white lung“ +/- subpleural consolidation = 2 points; extensive consolidation +/- „white lung“, lung tissue looks as a solid organ = 3 points. Furthermore, the points were calculated (maximum score = 36 points). In addition to the calculation of points, a search was performed in each of the zones for the signs corresponding to complications or associated conditions (exudative pleurisy, respiratory distress syndrome, pneumothorax, lung atelectasis, pulmonary edema), which were noted as additional profiles of pathological changes (complications): pneumothorax; no pleura sliding; pleural effusion; lung pulse; lung points. The selected 12 zones corresponded to the subpleural areas of the anatomical segments indicated in Tab. 2.

Statistical processing of the results was performed in the Windows-XP operating system, using the STATISTICA 6.0 application package (Stat Soft, GS-35F-5899H; USA) and MedCalc (version 9.6.2.0; Belgium). Since the distribution of the data differed from normal, we used the methods of nonparametric statistics: median (Me), minimum (Min) and maximum (Max) values, 25th (Q1) and 75th (Q3) percentiles, 95% confidence interval (95% CI). The correlation of quantitative features was assessed by the Spearman method with the determination of the rank correlation coefficient. Receiver operating characteristic (ROC) curves were plotted to determine the informative

Tab. 3. Comparative characteristics of some parameters of patients with COVID-19 infection with and without pneumonia

Variables	Patients with pneumonia n = 25	Patients without pneumonia n = 14	U/ χ^2	p
Age, years, Me [Q1; Q3]	49 [31; 75]	48 [32; 69]	139.0	0.291
Gender, male/female (%)	10(40)/15(60)	7(50)/7(50)	0,36	0.546
Symptoms duration, days Me [Q1;Q3]	8 [3;23]	12 [6;60]	111.0	0.062
Symptoms:				
fever	23	12	1.23	0.608
dyspnea	11	6		0.945
cough	17	7		0.268
sputum	7	4		0.624
anosmia	6	0		0.054
Comorbidities	15	8	0.03	0.862

value of the research method. A comparison was made with the reference method to assess the diagnostic value of LUS. Differences at the $p < 0.05$ level were considered statistically significant.

Results and discussion

According to CT data, 25 out of 39 patients included in the study (64%; 95% CI 47–79) were diagnosed with pneumonia, which, in accordance with the criteria, was regarded as COVID-19 associated. Some demographic and clinical parameters of patients are presented in Tab. 3.

Patients in the compared groups did not have statistically significant differences in the basic parameters. We observed a tendency for a longer period of clinical symptoms of the infectious process in the group without pneumonia, which was probably due to the presence of 3 patients with

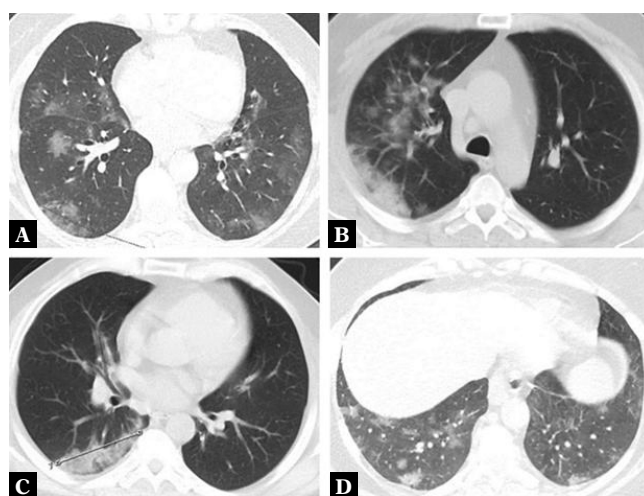


Fig. 1. Prevalent lung lesions patterns in COVID-19-associated pneumonia in computed tomography: **A.** Areas of ground-glass opacities, mainly subpleural. **B.** Different-sized areas of ground-glass opacities with unilateral subpleural consolidation. **C.** Widespread subpleural infiltration with consolidation. **D.** Multiple bilateral small areas of ground-glass opacities with consolidation foci

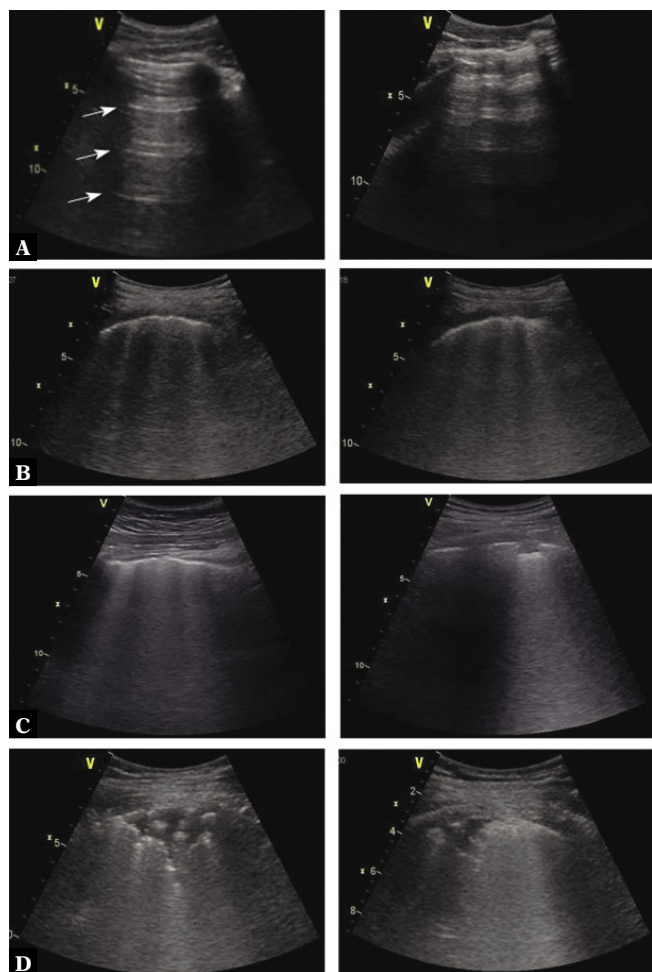


Fig. 2. Prevalent profiles of lung lesions in COVID-19-associated pneumonia in lung ultrasound **A.** Norm (A-lines, score = 0). **B.** Narrow B-lines, more than 3 in one zone (score = 1). **C.** Coalescent wide B-lines. Subpleural consolidation, discontinuous pleural line (score = 2). **D.** Large consolidated area, white lung phenomenon (score = 3)

chronic bronchitis in this group. Patients with pneumonia were more likely to report anosmia among complaints. The main symptoms of COVID-19 infection in both groups were fever, cough, and dyspnea.

Patients with pneumonia detected by CT had typical signs of pulmonary involvement in COVID-19 according to CO-RADS⁽³⁾. The median parenchymal lesion spread measured by visual assessment was 30% (Q1 = 14; Q3 = 40).

Tab. 4. Receiver operating characteristic of different cut-off at lung ultrasound score for diagnosis of COVID-19 associated pneumonia

Lung ultrasound score	Se, %	95% CI	Sp, %	95% CI	PPV, %	NPV, %
≥0	100.00	86.3–100.0	0.00	0.0–23.2	64.1	
>0	100.00	86.3–100.0	57.14	28.9–82.3	80.6	100.0
>1	96.00	79.6–99.9	64.29	35.1–87.2	82.8	90.0
>2	88.00	68.8–97.5	100.00	76.8–100.0	100.0	82.4

Bilateral lesions were found in 92% of cases (95% CI 74–99). The most common CT signs were multifocal, subpleural and/or bilateral “ground glass” opacities located along the interlobar pleura, and areas of subpleural consolidation (Fig. 1).

All 25 patients with CT confirmed pneumonia had LUS signs of interstitial changes in the lung parenchyma. The most common LUS interstitial signs were as follows: multiple (narrow) B-lines, confluent (wide) B-lines, as well as areas of subpleural consolidations and “white lung” (Fig. 2). Minor pleural effusion was found in only 2 patients with pneumonia. In 6 patients, lung ultrasound showed signs of interstitial lesions, which were not confirmed by the chest CT. Of these, LUS signs were represented by narrow B-lines (lower lateral surface on the left and right) in 4 cases, and a single area of insignificant subpleural consolidation in 2 cases. Changes in the last two cases were studied in more detail and compared with chest CT images. In one case (57-year-old female patient), an intraorgan lymph node measuring 5 mm was detected in the zone of LUS changes (Fig. 3A, Fig 3B); in another case, a 38-year-old man had a linear fibrosis area in the lower lobe of the left lung (Fig. 3C). In all 6 cases, the score was 2; clinically, the patients had complaints and signs of mild respiratory disease. In two other patients, after 7 and 10 days of illness (respectively), repeated chest CT scans confirmed pneumonia. We do not know if these changes in the lungs were a new process or if ultrasound of the lungs is more sensitive than CT for COVID-associated lung lesions.

Only two patients had a significant lung tissue lesion according to CT scan (lesion volume up to 60%). LUS signs in these cases included areas of extensive consolidation, confluent B-lines with the formation of the of “white lung” phenomenon

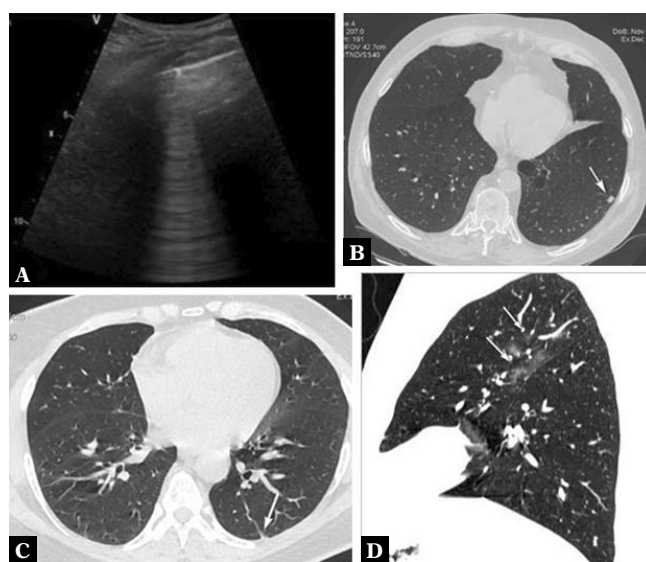


Fig. 3. **A, B.** Intrapulmonary lymph node: echoscopic image (left) and tomogram (right). **C.** Area of linear fibrosis. **D.** Areas of infiltration along the interlobar pleura, not detected by lung ultrasound

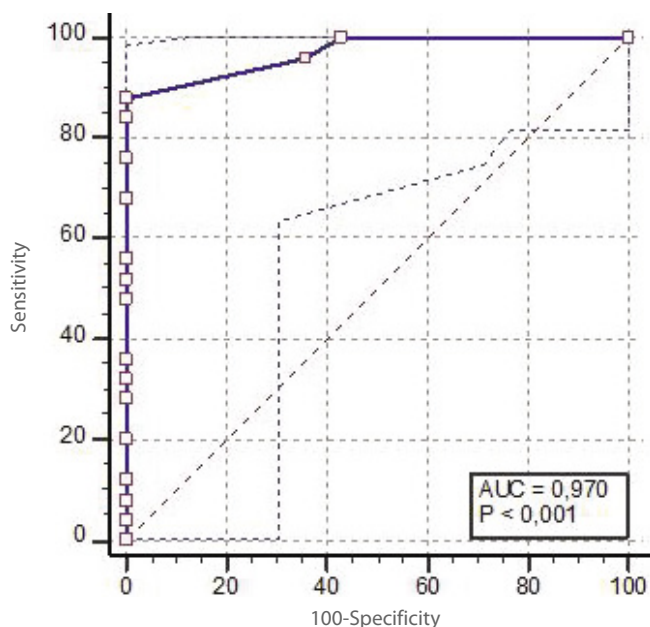


Fig. 4. Cut-off value for lung ultrasound in detecting pneumonia associated with COVID-19 infection

(LUS score 22 and 24 out of 36). Clinical signs included dyspnea, tachypnea, low oxygen saturation (below 90%).

Furthermore, a ROC-curve was plotted in order to determine the cut-off that optimally reflects the Se/Sp ratio for LUS score (Fig. 4).

As the analysis showed, the cut-off point of ≥ 2 had the optimal sensitivity (Se)/specificity (Sp) ratio: Se = 88.0% (95% CI 68.8–97.5), Sp = 100.0% (95% CI 76.8–100.0). The area under the curve (AUC) was 0.970 (95% CI 0.858–0.999; $p < 0.0001$), which corresponds to an excellent model. The probability of detecting pneumonia at a value of ≥ 2 points is 100% (positive predictive value (PPV) = 100%). The negative predictive value (NPV) was 100%.

The results of determining the Se, Sp, PPV and NPV of the method with different values of the sum of points are shown in Tab. 4.

Furthermore, the changes revealed by CT were compared according to the anatomical areas examined by ultrasound of the lungs. For each of the CT-areas, a score was given for the lesion of the pulmonary parenchyma. Correlation analysis between scores for lung ultrasound and chest CT was performed. The scatter plot of the objects of study in coordinates is shown (Fig. 5).

The LUS score showed a significant positive correlation with CT visual score ($r = 0.928$, 95% CI 0.867–0.962, $p < 0.001$). Correlation analysis results, along with the results of the ROC analysis, are needed to consider the LUS method acceptable for assessing pulmonary parenchyma lesions in patients with COVID-19 associated pneumonia, including an assessment of the extent of the spread of the pathological process.

Limitations

The most obvious limitation of our study is the small sample size. We believe that the study needs to be continued to dynamically assess pulmonary lesions in patients with COVID-19 pneumonia.

The inability to detect deep lung tissue lesions is a limitation of LUS. On the other hand, COVID-19 mostly affects the peripheral subpleural regions. In practice, however, we can face a completely opposite situation (Fig. 3D). Such areas may be visualized only in the case of a significant loss of airiness in the subpleural regions due to massive consolidation. In addition, the left and right segments S7 are completely inaccessible for echoscopic examination.

Some LUS signs found in COVID-19-associated pneumonia can occur in a number of other pathological processes in the pulmonary parenchyma – pneumonia of a different etiology (including bacterial), respiratory distress syndrome, left ventricular failure, atelectasis, abscess, fibrosis (including post-inflammatory)⁽¹⁰⁾. Thus, a decrease in the positive predictive value of LUS is likely to be expected with a decrease in the incidence of COVID-19 infection and the associated lung tissue damage. When evaluating study results, it is extremely important to assess the clinical data and the epidemiological situation^(7,11). In our study, we evaluated the method in a group of patients with laboratory-confirmed COVID-19 infection. In our opinion, it is more essential to study the results using LUS in other patient populations, for example, before performing laboratory tests for SARS-CoV-2, as well as in persons without clinical signs of COVID-19 infection (asymptomatic course).

Conclusion

For LUS in outpatients with COVID-19-associated pneumonia the optimal Se/Sp ratio had a cut-off point of ≥ 2 points: Se = 88%, Sp = 100%, AUC = 0.970 (95% CI 0.858–0.999; $p < 0.0001$).

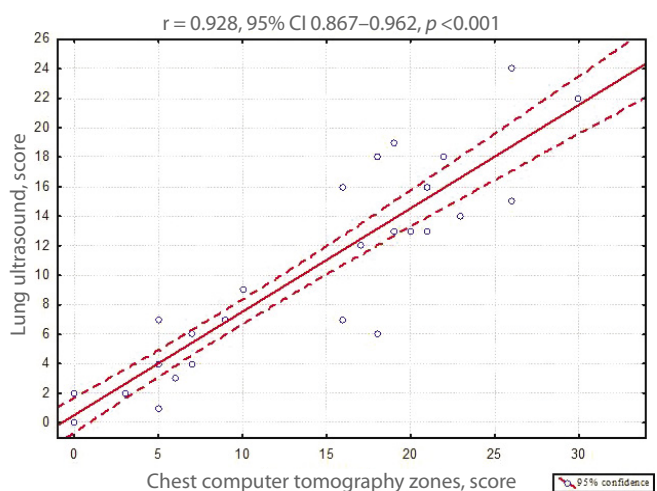


Fig. 5. Correlation between lung ultrasound score and computed tomography positive zone score

The preliminary analysis of the obtained data demonstrated that the LUS method can be useful for detecting changes in COVID-19 infection with mild-to-moderately severe pneumonia as confirmed by a CT chest scan. The obtained results are probably due to the typical localization of interstitial changes in the lungs in this type of viral infection. The LUS score correlated with the chest CT score ($r = 0.928$, 95% CI 0.867–0.962, $p < 0.001$).

LUS can be extremely useful in primary care setting, in the absence of a CT scanner, in an intensive care unit, and for point-of-care diagnostics. At the same time, further study of this method in heterogeneous populations is needed, as well as validation of the method for other interstitial lung diseases.

Conflict of interest

The authors declare no conflict of interest.

Financing

The study was performed without external funding.

Conformity with the principles of ethics

The study was approved by the local ethics committee, protocol No. 8 dated 10/12/2020.

References

1. Borakati A, Perera A, Johnson J, Sood T: Chest X-ray has poor diagnostic accuracy and prognostic significance in COVID-19: a propensity matched database study. *BMJ Open* 2020; 10: e042946.
2. Cardinale L, Priola AM, Moretti F, Volpicelli G: Effectiveness of chest radiography, lung ultrasound and thoracic computed tomography in the diagnosis of congestive heart failure. *World J Radiol* 2014; 6: 230–237.
3. Prokop M, van Everdingen W, van Rees Vellinga T, Quarles van Ufford H, Stöger L, Beenen L *et al.*: CO-RADS: a categorical CT assessment scheme for patients suspected of having COVID-19-definition and evaluation. *Radiology* 2020; 296: E97–E104.
4. Walker CM, Chung JH: Müller's Imaging of the Chest. Second ed. Elsevier, Philadelphia 2019.
5. Rubin GD, Ryerson CJ, Haramati LB, Sverzellati N, Kanne JP, Raoof S *et al.*: The role of chest imaging in patient management during the COVID-19 pandemic: a multinational consensus statement from the Fleischner society. *Chest* 2020; 158: 106–116.
6. Lichtenstein D., Meziere G., Seitz J.: The dynamic air bronchogram. A lung ultrasound signs of alveolar consolidation ruling out atelectasis. *Chest* 2009; 135: 1421–1425.
7. Soldati G, Smargiassi A, Inchingolo R, Buonsenso D, Perrone T, Briganti DF *et al.*: Proposal for international standardization of the use of lung ultrasound for patients with COVID-19: a simple, quantitative, reproducible method. *J Ultrasound Med* 2020; 39: 1413–1419.
8. World Health Organization. WHO Guidelines for the collection of human specimens for laboratory diagnosis of avian influenza infection. Available at: https://www.who.int/influenza/human_animal_interface/virology_laboratories_and_vaccines/guidelines_collection_h5n1_humans/en/.
9. Oikonomou A, Prassopoulos P: Mimics in chest disease: interstitial opacities. *Insights Imaging* 2013; 4: 9–27.
10. Buda N, Kosiak W, Welnicki M, Skoczylas A, Olszewski R, Piotrkowski J *et al.*: Recommendations for lung ultrasound in internal medicine. *Diagnosics (Basel)* 2020; 10: 597.
11. Buda N, Cylwik J, Kwiecińska R: Similarity of lung ultrasound image in patients with COVID-19 and COVID-19-like illnesses. *Am J Respir Crit Care Med* 2021; 203: 628–629.